Electron Transport and Back Reaction in Electrochemically Self-Assembled Nanoporous ZnO/Dye Hybrid Films

T. Oekermann,[†,‡] T. Yoshida,[*,†] H. Minoura,[†] K. G. U. Wijayantha,[§] and L. M. Peter[§]

Gifu University, Graduate School of Engineering, Yanagido 1-1, Gifu 501-1193, Japan, University of Hannover, Institute of Physical Chemistry and Electrochemistry, Callinstrasse 3-3A, 30167 Hannover, Germany, and University of Bath, Department of Chemistry, Bath BA2 7AY, U.K.

Received: December 12, 2003; In Final Form: March 6, 2004

Nanoporous ZnO/eosinY films prepared by electrochemical self-assembly have already shown promising characteristics for use in dye-sensitized solar cells, such as ease of preparation (no need for high-temperature sintering) and high dye loading. In this study, electron transport and back reaction in these films have been investigated by intensity modulated photocurrent spectroscopy (IMPS) and intensity-modulated photovoltage spectroscopy (IMVS). In contrast to sintered colloidal ZnO films, electrodeposited ZnO/eosinY films exhibit electron transit times (τ_D) that are much shorter than electron lifetimes (τ_n), leading to very efficient electron collection. The shorter transit times in the electrodeposited layers are due in part to the fact that the films are very thin, but in addition the electron diffusion coefficients are higher than in sintered colloidal ZnO films. Although the unusually high dye concentration in the electrochemically self-assembled film allows efficient light harvesting, it was found that not all dye molecules inject electrons. The low injection efficiency is probably due to the formation of dye aggregates.

Introduction

In recent years, one-step electrodeposition of ZnO from aqueous zinc salt solutions in the presence of water-soluble dyes has been shown to provide a valuable route for the preparation of new inorganic/organic hybrid materials.[1] The various dye molecules such as tetrasulfonated metallophthalocyanines,[2,3] tetrabromophenol blue,[4] and eosinY[5−7] influence the ZnO deposition, giving rise to a variety of film structures and morphologies, depending on the preparation conditions, e.g., the electrode potential and the kind of dye used. While in some cases the majority of the dye molecules end up trapped between[3] or in[7] the ZnO crystals, in most cases porous ZnO films with dye molecules adsorbed on the ZnO surface are formed. These materials are ideal candidates for a use in dye-sensitized solar cells. In fact, these films perform as sensitized photoanodes when they are soaked in an I^-/I_3^- redox electrolyte and illuminated with visible light.[3−7] As the deposition method requires no heat treatment, it also provides a synthetic route for fabrication of solar cells on flexible plastic substrates.

The highest photocurrents for this kind of electrodeposited ZnO/dye films have been found when eosinY was used as the dye, especially when deposited from oxygen saturated $ZnCl_2$ solutions at potentials <-0.9 V vs SCE.[7] Under these conditions, the eosinY molecules are reduced and form a stable complex with Zn^{2+}.[6] The complex strongly adsorbs on the ZnO surface, causing the formation of nanoporous, spongelike ZnO crystals with a very high dye loading. Short-circuit photocurrents between 2 and 3 mA cm^{-2} have been found under white light illumination ($\sim$1 sun) for the as-deposited films without further treatment.[7]

In this study, the photoelectrochemical properties of these ZnO/eosinY hybrid films have been investigated in more detail in view of their potential applications in dye-sensitized solar cells. One way to measure the performance of solar cells for a certain wavelength of the incident light is the incident photon to current conversion efficiency (IPCE), which can be described by the equation

$$\mathrm{IPCE}\ (\lambda) = \mathrm{LHE}\ (\lambda)\Phi_{inj}\eta_c \qquad (1)$$

where LHE stands for the light harvesting efficiency, Φ_{inj} is the efficiency of electron injection, and η_c is the collection efficiency of injected electrons. While a high LHE can be assumed for the electrodeposited ZnO/eosinY films due to their high dye loading,[7] the other two factors still have to be investigated. The main topic of the present study is the collection efficiency of injected electrons, which was studied in detail using intensity modulated photocurrent spectroscopy (IMPS) and intensity modulated photovoltage spectroscopy (IMVS). IMPS and IMVS are powerful tools to investigate transport and back-reaction kinetics of photogenerated electrons in nanoporous films, since the electron lifetime τ_n, the mean electron transit time τ_D, and the effective electron diffusion coefficient D_n can be obtained.[8] The relative values of τ_n and τ_D determine the collection efficiency of injected electrons; τ_n should be significantly larger than τ_D for efficient electron collection. In this study, τ_n and τ_D values for electrochemically self-assembled ZnO/eosinY films were compared with the values for sintered colloidal nanoporous ZnO films sensitized with eosinY.

Theory

In the limit of small amplitude light perturbations, the generation and collection of electrons in dye-sensitized nanocrystalline solar cells can be described by the continuity

* Corresponding author. E-mail: yoshida@apchem.gifu-u.ac.jp.
[†] Gifu University.
[‡] University of Hannover.
[§] University of Bath.

10.1021/jp037831m CCC: $27.50
Published on Web 05/20/2004

equation[8,9]

$$\frac{\partial n}{\partial t} = \Phi_{inj}\alpha I_0 e^{-\alpha x} + D_n\frac{\partial^2 n}{\partial x^2} - \frac{n - n_0}{\tau_n} \quad (2)$$

where α is the absorption coefficient, I_0 is the incident light intensity, D_n is the effective (intensity dependent) diffusion coefficient of electrons, n is the electron density under illumination, n_0 is the equilibrium electron concentration in the dark, and τ_n is the effective first-order electron lifetime (also intensity dependent). The electron lifetime is assumed to be determined by the back reaction of electrons with I_3^- in the electrolyte. Light scattering and any electric field in the film are usually neglected.[8,10]

During the IMVS and IMPS measurements the cell is illuminated with sinusoidally modulated light with a small ac component (10% or less of the dc component), which can be described by the periodic illumination function

$$I(t) = I_0[1 + (\delta e^{i\omega t})] \quad (3)$$

where $\omega = 2\pi f$ is the variable modulation frequency and δ is $\ll 1$. The photocurrent or photovoltage response is measured in terms of its amplitude and phase shift with respect to the illumination function, and it can be represented in the IMPS and IMVS complex plane plots.

On the basis of the illumination function in eq 3, analytical solutions of eq 2 for short-circuit (IMPS) and open-circuit (IMVS) conditions have been published in the literature.[8,11,12] The IMVS response is characterized by a semicircle in the positive/negative quadrant of the complex plane, and τ_n can be calculated directly from the IMVS response since $\tau_n = 1/\omega_{min} = 1/2\pi f_{min}$ where f_{min} is the frequency of the minimum of the semicircle, i.e., the frequency of the lowest imaginary component in the IMVS plot.[12] Correspondingly, an electron transit time $\tau_D = 1/\omega_{min} = 1/2\pi f_{min}$ can be defined for IMPS, which gives a convenient estimate of the average time that photoinjected electrons need to reach the back contact. It is comparable with the time taken for electrons to travel halfway through the film, which is given by $d^2/4D_n$ where d is the film thickness (exact calculations for illumination from the substrate side show that τ_D as defined here is between 1.3 and 1.5 times higher than $d^2/4D_n$ for $\alpha d < 5$). Using τ_n from the IMVS measurements, the analytical solutions of eq 2 derived by Dloczik et al.[11] can be used to fit the IMPS response and calculate the effective diffusion coefficient D_n of electrons. The normalized solution for the photocurrent j_{photo} and therefore the IMPS response for illumination through the back contact of the film are

$$\frac{j_{photo}}{q\delta\Phi_{inj}I_0} = \frac{\alpha}{\alpha + \gamma}\cdot\frac{e^{\gamma d} - e^{-\gamma d} + 2\alpha\dfrac{e^{-\alpha d} - e^{-\gamma d}}{\gamma - \alpha}}{e^{\gamma d} + e^{-\gamma d}} \quad (4)$$

with

$$\gamma = \left[\frac{1}{D_n\tau_n} + i\frac{\omega}{D_n}\right]^{1/2} \quad (5)$$

where q is the elementary charge and d is the film thickness.[11] The effective diffusion coefficient takes into account the possible trapping and detrapping of electrons. In the case of monoenergetic traps, it can be defined by

$$D_n = D_{cb}\frac{k_d}{k_t} \quad (6)$$

where k_t and k_d are the first-order rate constants for trapping and detrapping, respectively, and D_{cb} is the diffusion coefficient of electrons in the conduction band.[13] In the case of TiO_2 films, it appears that electron traps are distributed exponentially in energy, giving rise to a characteristic intensity dependence of D_n, which arises from trap filling.[14] An important advantage of small-amplitude methods such as IMPS and IMVS is that D_n as well as τ_n can be treated as constant for a given dc light intensity I_0.[11]

The experimentally measured IMPS response is affected by *RC* attenuation, especially toward higher frequencies. To obtain the attenuated response, eq 4 is multiplied with the complex attenuation function

$$A(\omega) = \frac{1}{1 + i\omega RC} \quad (7)$$

where R is the series resistance and C is the capacitance of the electrode.[15] It has been found that, under short circuit conditions, R and C are due to the $SnO_2|TiO_2$ and $SnO_2|$electrolyte interfaces with typical values of around 10 to 20 Ω and 30 μF cm^{-2}.[11,15]

Experimental Section

Film Preparation and Characterization. Details of the electrochemical self-assembly of ZnO/eosinY films from $ZnCl_2/O_2$ aqueous solution are given in ref 7. For the present study, ZnO films were electrodeposited from a solution containing 5 mM $ZnCl_2$ (Merck), 0.1 M KCl (Merck), and 50 μM eosinY disodium salt (Kanto Chemicals) that was saturated with oxygen and maintained at 70 °C. F-doped SnO_2 (FTO) coated conducting glass (Nippon Soda Glass, 20 Ω/sq) served as substrate after being degreased by ultrasonic cleaning in acetone and ethanol, etched in a 45% nitric acid, and finally rinsed with water. The electrodeposition was carried out at −1.4 V (vs MSE) for 20 min using an EG&G Princeton Applied Research Potentiostat/Galvanostat Model 273A, a 4N pure Zn wire as counter electrode and a mercurous sulfate electrode (MSE, E_{MSE} = +0.65 V vs NHE) as reference electrode. The deposited films were rinsed with water and dried under air at room temperature.

For comparison, colloidal ZnO films were prepared from a paste containing 1.5 g of ZnO powder (Tayka MZ 300, particle size 30 nm),1.5 g of zinc acetate, and 0.1 mL of acetic acid in 10 mL of ethanol. The paste was coated on FTO/glass by the doctor blade method and calcinated for 30 min at 450 °C. EosinY was adsorbed from a 0.5 M ethanolic solution for 24 h.

The films were prepared on 2.5 × 5 cm FTO/glass sheets, which were cut into electrodes with geometrical film areas of about 0.25 cm^2 each. The amount of the loaded dye was determined from the UV−vis absorption spectrum of a solution prepared by dissolving a known area of the films into a known volume of concentrated aqueous ammonia solution. Film thickness measurements were made with a Kosaka Laboratories SE-2300 tracing stylus surface profilometer.

Photoelectrochemical Measurements. Sandwich cells were fabricated using the ZnO/eosinY films as working electrodes and platinized FTO on glass as counter electrodes. The electrodes were placed face to face with pieces of thin Teflon tape as spacers (thickness about 10 μm) between them. The electrolyte was a mixture of ethylene carbonate and propylene carbonate (50:50 by weight) containing 0.4 M KI and 0.04 M iodine.

High-intensity green LEDs (530 nm), which provided dc light intensities up to 2.6 mW cm^{-2} (8.6×10^{15} photons s^{-1} cm^{-2}) at the electrodes, were used as light sources for IMPS and IMVS.

TABLE 1: Film Thicknesses, Geometric Dye Loadings (Amount of Loaded Dye per Geometric Electrode Area), and Dye Concentrations of the Films Used in This Study[a]

ZnO	film thickness (μm)	geometric dye loading (mol cm^{-2})	dye concn (mol L^{-1})
electrodeposited	1.4	8.8×10^{-8}	0.63
colloidal	10	6.6×10^{-8}	0.066

[a] For the calculation of the dye concentration in the film a homogeneous distribution of the eosinY in the films was assumed.

The sandwich cells were illuminated through the back contact of the ZnO, modulating the light intensities (±5%) by an ac voltage applied to the LED via a series resistor from the frequency response analyzer (FRA). The dc and ac light intensities were measured with a calibrated silicon photodiode. Neutral density filters were used to vary the light intensities down to about 0.05 mW cm^{-2}. Corrections were made for light absorption and reflection in the conductive glass substrates.

A Toho Technical Research 2000 potentiostat/galvanostat was used to measure open-circuit voltages for IMVS. The amplitudes and phase shifts of the voltage response with respect to the modulation of the light intensity were measured with an NF Electronic Instruments S-5720C FRA. For IMPS, a homemade operational amplifier potentiostat specially constructed for fast measurements and a Solartron 1250 frequency response analyzer were used. In both cases, the control of the FRA and the data acquisition during a series of measurements were carried out using a personal computer.

For comparison, separate IPCE measurements were made using an Ushio 500 W Xe arc lamp and a Nikon G 250 monochromator. The wavelength was varied with 10 nm intervals between 400 and 650 nm, and the light intensity was measured for each wavelength using a calibrated Eppley thermopile. The IPCE was calculated by dividing the flux of photogenerated electrons by the photon flux. The photon fluxes varied between 4×10^{14} s^{-1} cm^{-2} and 6×10^{14} s^{-1} cm^{-2}, with a value of 5.6×10^{14} s^{-1} cm^{-2} at 530 nm.

Results

The film thicknesses, dye loadings, and dye concentrations of the films used in this study are shown in Table 1. Compared to the colloidal film, the electrodeposited ZnO/dye film was very thin and had a very high dye concentration as reported earlier.[7] The amount of loaded dye in the film is comparable in both cases, which means that both kinds of film should have similar light harvesting efficiencies (LHE).

Figure 1 shows typical complex plane IMPS and IMVS plots measured at electrodeposited ZnO/eosinY electrodes. The IMPS plots in Figure 1a are flattened semicircles, as expected for a distribution of electron transit times. While eq 4 would predict an IMPS plot fully within the positive/negative quadrant,[11] the plots in Figure 1a cross the imaginary axis toward higher frequencies, so that parts of the plots appear in the negative/negative and negative/positive quadrants. This behavior has been predicted for illumination from the electrolyte side in the case of a low penetration depth of the light, caused by slow electron transport through the film,[16] but it is not expected for illumination from the substrate side where electrons are photogenerated rather near to the back contact.[8] In the latter case, the crossing of the imaginary axis may be caused by *RC* attenuation (eq 7) or by an inhomogeneous dye distribution in the film.[15] However, an inhomogeneous dye distribution is not expected for the electrochemically self-assembled films, since the ZnO and the dye are deposited simultaneously throughout the deposition process. Moreover, no significantly different dye concentrations were found in films deposited in different deposition times under otherwise constant conditions.[17] Therefore, it is likely that the crossing of the imaginary axis is caused by *RC* attenuation, which will be further discussed below.

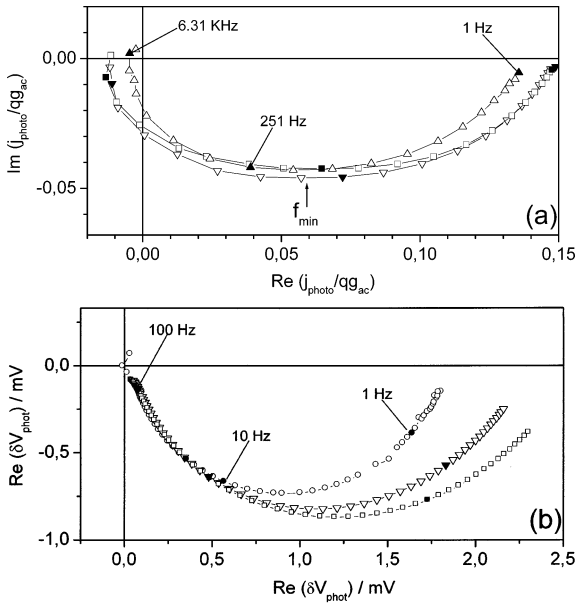

Figure 1. (a) Typical IMPS plots of an electrodeposited ZnO/eosinY electrode. The film was illuminated with dc light intensities of 0.89 mW cm^{-2} (▽), 0.50 mW cm^{-2} (□), and 0.29 mW cm^{-2} (△). The solid symbols (▼, ■, ▲) indicate measurements at 6.31 KHz, 251 Hz, and 1 Hz. The axes show normalized photocurrents (electron flux/photon flux), so that the amplitudes correspond to the ac component of the IPCE. (b) IMVS plots of the same film measured at light intensities of 2.6 mW cm^{-2} (○), 0.8 mW cm^{-2} (▽), and 0.4 mW cm^{-2} (□) between 0.2 and 200 Hz. The solid symbols (●, ▼, ■) indicate measurements at 100, 10, and 1 Hz.

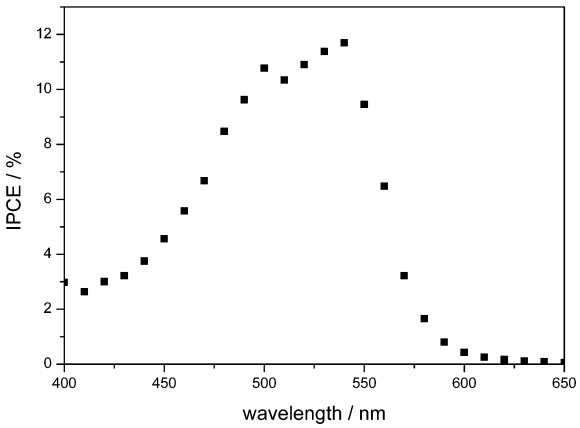

Figure 2. Photocurrent action spectrum of an electrodeposited ZnO/eosinY film.

Since normalized photocurrents are shown in Figure 1a, the real components of the low-frequency limits of the IMPS plots equal the differential IPCE. The differential IPCEs of 14−15% for the higher light intensities seen in Figure 1a are in good accordance with IPCE values obtained from separate dc measurements. One example of the photoaction spectrum of an electrodeposited ZnO/eosinY film is shown in Figure 2. The two maxima in the photoaction spectrum are in accordance with the maxima seen in absorption spectra of electrodeposited ZnO/eosinY films published earlier.[6] The IPCE values for 530 nm

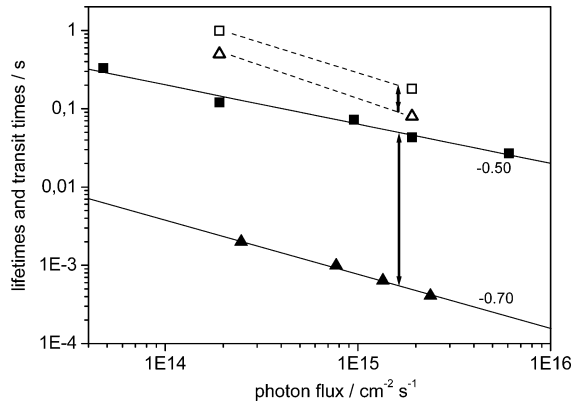

Figure 3. Electron transit times τ_D and lifetimes τ_n for an electrodeposited ZnO/eosinY film at different dc light intensities (τ_D = ▲; τ_n = ■). Transit times and lifetimes for a colloidal ZnO/eosinY film (τ_D = △; τ_n = □) are shown for comparison. Solid lines were calculated by linear regression with the slopes given in the plot. The 2 arrows indicate the differences between τ_D and τ_n for both kinds of films.

in Figure 2 (11.4%) is comparable with the values obtained from Figure 1a.

The IMVS plots in Figure 1b show decreasing values of δV_{photo} toward higher light intensities. This is consistent with the finding at nanoporous TiO_2 electrodes that the photovoltage increases rather steeply with the light intensity in the range of lower light intensities, while a relatively weak light intensity dependence is observed in the range of higher light intensities.[13] The values of $f_{\min}$ increase toward higher light intensities, indicating a decreasing electron lifetime τ_n. The same behavior is seen for $f_{\min}$ and therefore the electron transit time τ_D in Figure 1a. The light intensity dependence of these values is further analyzed in Figure 3.

Figure 3 is a summary of the results of IMPS and IMVS measurements at electrodeposited as well as colloidal films, including the results of the plots shown in Figure 1. The double logarithmic plot shows how the electron lifetimes τ_n and transit times τ_D, calculated from the $f_{\min}$ values of the IMVS and IMPS plots, depend on the light intensity. A slope of -0.70 is found for the light intensity dependence of τ_D of the electrodeposited film, which is similar to previous results for nanoporous dye-sensitized TiO_2 films.[13,17,18] The decrease in transit time at higher intensities can be explained by a higher trap occupancy, which leads to a higher effective diffusion coefficient because only shallow traps are able to retard electrons. For the light intensity dependence of τ_n a slope of -0.5 is obtained. This means that τ_n is inversely proportional to the square root of the light intensity. Such light intensity dependence has already been reported for dye-sensitized nanocrystalline TiO_2 and attributed to second-order back-reaction kinetics.[13]

Two main aspects can be extracted from the results in Figure 3. First, τ_D for the electrodeposited films is found to be smaller than τ_D of the colloidal film by more than 2 orders of magnitude. This result is consistent with earlier photocurrent transient measurements in the ms regime. Those measurements showed a very fast increase of the photocurrent, compared to colloidal ZnO, upon the beginning of illumination.[7] One reason for this faster charge collection can be seen in the lower thickness of the electrodeposited film (Table 1). Random walk diffusion predicts that the transit time from any point in the film at a distance x from the substrate is given by

$$\tau_D = x^2/D_n \tag{8}$$

However, the difference in the film thickness would only explain a difference in the transit times of a factor of 50. Therefore, the results also suggest that electron transport is faster in the electrodeposited film. Second, compared to the differences in τ_D, the differences in the electron lifetimes τ_n of the two kinds of film are much less significant. This leads to a much larger difference between τ_n and τ_D of the electrodeposited film, compared to the difference between these values for the colloidal film. In fact, τ_n and τ_D of the colloidal film only differ by a factor of about 2, which already shows that not all photogenerated electrons injected into the ZnO are collected at the back contact, if a certain distribution of τ_n and τ_D is assumed. On the other hand, a difference between τ_n and τ_D of nearly 2 orders of magnitude, as it is seen for the electrodeposited ZnO, should lead to an electron collection efficiency of practically 100%. This suggests that the rather low IPCE, which is found for electrodeposited ZnO (Figures 1a and 2) is caused by a low electron injection efficiency Φ_{inj}. Electron injection and transport will be discussed in detail in the following chapter.

Discussion

For a more detailed comparison of the electron-transport properties of the two kinds of ZnO film investigated in this study, the different film thicknesses and dye concentrations in the films have to be considered. Therefore, values of the diffusion coefficients D_n were obtained by comparing the experimental IMPS responses with plots calculated using eq 4. Setting $\Phi_{inj} = 1$, fixed experimental values of τ_n, α, and d were used in the theoretical calculation and D_n was varied until it yielded the f_{min} values obtained in the experiments.[13,18] However, a comparison of the low frequency intercepts of the theoretical and experimental plots immediately showed that the experimental IMPS plots give much lower intercepts and therefore IPCE values than expected for $\Phi_{inj} = 1$. Furthermore, even if Φ_{inj} was set to lower values, no good fits could be obtained especially toward higher frequencies, which points toward an influence of the *RC* constant.

To obtain fits which better represent the experimental curves and also consider the influence of the *RC* constant, eq 4 was multiplied with eq 7, and the result was split into its real and imaginary components as functions of the frequency *f*. Fitting routines for least-squares fits were written for these two functions, and the experimental results were then fitted by simultaneously varying D_n, Φ_{inj}, R and C, while again experimental data were inserted for τ_n, α and d. To evaluate the role of the *RC* attenuation, fits were also made by varying D_n and Φ_{inj} only and inserting 0 for R and C, respectively. The example in Figure 4 shows that rather good fits were obtained over the whole frequency range if *RC* attenuation was considered, while significant deviations occurred at higher frequencies if *RC* attenuation was neglected. This clearly shows that the deviations in the IMPS plots, which are seen in Figure 1a toward higher frequencies, are caused by *RC* attenuation.

For both the electrodeposited and the colloidal films the fits of the IMPS results gave values around 5 μF for C and 20 Ω for R. These values are in good accordance with the findings of others,[11,15] which suggests that R and C are due to the conducting substrate also in the present study. This is further supported by a comparison with the surface resistivity of the conducting material (20 Ω/sq) and with separate capacity measurements at other colloidal and electrodeposited ZnO/eosinY films on the same kind of substrate. The latter showed values between 4.4 and 9.2 μF for electrodeposited films and

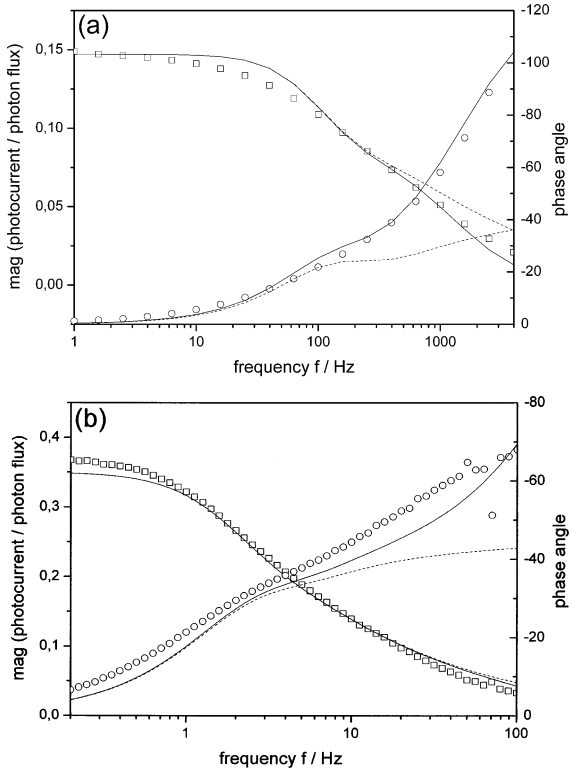

Figure 4. Experimental values of |IPCE| (□) and phase angles (○) and their simulation by least-squares fits (—). Films, light intensities, and parameters for the fits: (a) electrodeposited ZnO/EY, 2.38×10^{15} photons cm^{-2} s^{-1}, $\alpha = 19\,700$ cm^{-1}, $D_n = 4.4 \times 10^{-6}$ cm^2 s^{-1}, $R = 20$ Ω, $C = 5 \times 10^{-6}$ F, $\Phi_{inj} = 0.16$; (b) colloidal ZnO with EY adsorbed from solution, 1.91×10^{15} photons cm^{-2} s^{-1}, $\alpha = 800$ cm^{-1}, $D_n = 2.4 \times 10^{-6}$ cm^2 s^{-1}, $R = 20$ Ω, $C = 5 \times 10^{-6}$ F, $\Phi_{inj} = 1$. The dotted lines (- - -) show the respective fitting curves with $R = 0$ and $C = 0$ to show the influence of *RC* attenuation.

values of 5.2 and 6.8 μF for colloidal films. The deviations are probably caused by fluctuations in the roughness of the FTO layers.

The results also show that the electrodeposited ZnO/dye films are free of any electric field like it is known for nanoparticulate colloidal films because a field in these films should have lead to a higher *C*. Moreover, an electric field in the electrodeposited ZnO film would lead to a potential dependence of f_{min} in the IMPS measurements. In separate potential dependent IMPS measurements in a three-electrode setup (not shown), it was ensured that this is not the case. This result is actually not surprising because a porous structure with dimensions that are much smaller than the width of a space charge layer should always be totally depleted and free of an electric field.[19] The dimensions of the porous structure in the electrodeposited ZnO/dye films are not known exactly yet, however, from the higher dye loading of the electrodeposited films it can be assumed that they are probably even smaller than in the colloidal films.

The electron diffusion coefficients D_n, which were obtained from the best fits of the IMPS plots, are shown in Figure 5 for electrodeposited as well as colloidal ZnO/eosinY films. The values are shown against the dc photocurrent instead of the light intensity. Taking the dc photocurrent as a measure for the concentration of excess electrons in first approximation, this enables a better comparability of the electron transport properties since the occupancy of the traps in the ZnO, which is of high influence on D_n, depends on the excess electron concentration in the film. Significantly faster electron transport is therefore indicated for electrodeposited ZnO/eosinY compared to the

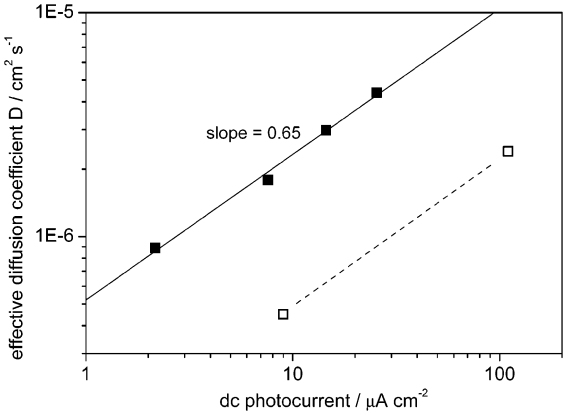

Figure 5. Effective electron diffusion coefficients D_n for a ZnO/eosinY film calculated by fitting the IMPS plots (■). D_n values for a colloidal ZnO/eosinY film (□) are shown for comparison. The solid line was calculated by linear regression.

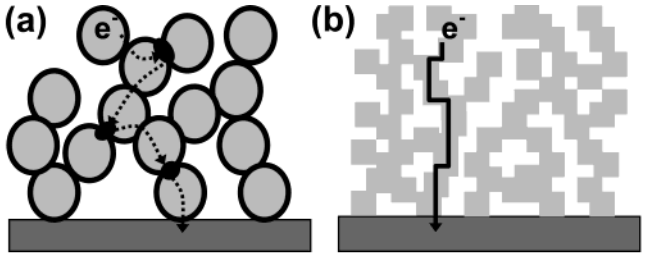

Figure 6. Simple qualitative model for the comparison of the electron transport in (a) colloidal ZnO and (b) electrodeposited ZnO. The black points at the grain boundaries in (a) indicate electron traps.

colloidal film. The difference amounts to a factor of ca. 4 in Figure 5, and there is still a difference by a factor of ca. 2 if the D_n values are plotted against the light intensity (not shown). The latter is in accordance with the results in Figure 3, where it was already shown that the difference in the film thickness cannot fully explain the differences in the τ_D values of the two films but that there has to be another reason such as faster electron transport in the electrodeposited film.

The electron diffusion coefficients presented in this paper are comparable with electron diffusion coefficients of sintered nanoporous TiO_2 films in a large number of publications. In a recent paper, Nakade et al.[21] compare electron diffusion coefficients of such films obtained by different experimental and analytical methods in their group and by others. For example, diffusion coefficients between 3×10^{-6} and 1.5×10^{-5} cm^2 s^{-1} are presented in that paper at a dc photocurrent of 100 μA cm^{-2}. The values found for the ZnO films in this study (2.5×10^{-6} cm^2 s^{-1} for the colloidal film, 10^{-5} cm^2 s^{-1} for the electrodeposited film estimated from Figure 5) are in the same range.

The fast electron transport in the electrodeposited film is quite remarkable, since is known for nanoporous TiO_2 that films prepared without high-temperature sintering show a significantly slower electron transport compared to films sintered at high temperatures.[21,22] However, no high temperatures are used in the electrodeposition of ZnO/eosinY films, while the colloidal ZnO films can be expected to show an even slower electron transport if sintered at lower temperature. Figure 6 illustrates the possible reasons for the faster electron transport in electrodeposited ZnO. Grain boundaries and electron traps, which are often located at grain boundaries, are present in the colloidal film (Figure 6a). As electrons spend some time in traps, the effective diffusion coefficient D_n becomes smaller if the trap density becomes higher.

TABLE 2: Comparison of the Efficiencies of Colloidal and Electrodeposited ZnO/EosinY Films in Sandwich Cells[a]

ZnO	η (%)	IPCE (%)
electrodeposited	0.8	15
colloidal	1.5	28

[a] For both kinds of film the overall light to electricity conversion efficiencies η for 20 mW cm^{-2} white light illumination and the incident photon to current conversion efficiencies (IPCE) for illumination with monochromatic light (530 nm, 10^{16} photons cm^{-2} s^{-1}) are shown. The values are maximum values obtained for a series of separate measurements at different films of each kind.

The conditions for electron transport in the electrodeposited films seem to be significantly different, which can also be derived from XRD measurements of the films and observation of its internal structure with TEM.[7] XRD confirmed a high crystallinity of the ZnO and a high level of preferential orientation with the *c*-axis perpendicular to the substrate as schematically shown in Figure 6b. It has been shown before that an ordered film structure can lead to an improvement in the electron transport properties[23] as it is the case for this material. TEM revealed a kind of fibrous structure, and the SAED patterns suggested the existence of micrometer-sized single crystalline domains containing nanometer-sized pores. Figure 6b reflects the smaller pore size and higher surface area of the electrodeposited film, which can also be derived from the much higher dye loading (Table 1). Note that Figure 6b represents only a section of just one of the large single crystalline domains which can be described as porous single crystals or sponge crystals.[7] Photoinjected electrons have to pass no or much less grain boundaries in these films on their way to the back contact (Figure 6b), and a lower trap density can be assumed for the electrodeposited film, which leads to a higher effective diffusion coefficient D_n.

It can be concluded at this point that, compared to colloidal films, the electrodeposited ZnO/eosinY films show a high electron collection efficiency due to both a very high dye concentration in the film, which enables the use of very thin films while still ensuring an efficient light harvesting, and better electron transport properties. However, sandwich cells based on electrodeposited ZnO/eosinY turned out to show lower efficiencies than those based on colloidal ZnO (Table 2). As already proposed above, a low injection efficiency can be the only reason for this observation because the LHE should be comparable for both films due to their similar dye loadings (Table 1). This is also strongly supported by the results of the fitting of the IMPS results: The best fits for the electrodeposited films were obtained with Φ_{inj} values in the range of the IPCE of the films. For the example shown in Figure 4a, the fitting yielded $\Phi_{inj} = 16\%$, while the IPCE was ca. 15% (Figure 1a). This finding clearly shows that the photocurrent of the electrodeposited film is limited by the electron injection efficiency and (to a much lower extent) by the LHE, but not at all by electron transport and collection.

Interestingly, the fits for the colloidal films always gave $\Phi_{inj} = 1$, even if the fitting sessions were started with lower values. Since the IPCE for these films is much lower than the LHE, it can be concluded that the photocurrent is limited by electron transport and collection in these films, as already seen in the small difference between τ_D and τ_n (Figure 3).

To discuss the low electron injection efficiency for electrodeposited films further, it should be noted that the films actually lost some of the dye if they were kept in the electrolyte for longer time (several hours). Contrary to the expectation that fewer dye molecules should lead to fewer photogenerated electrons, the photocurrent and efficiency of the film actually increased after a part of the dye was desorbed from the film (not shown). This leads to the conclusion that some of the dye molecules cannot inject electrons into the ZnO, and that these molecules are not adsorbed strongly in the film. Probably they are not adsorbed on the surface of the ZnO but form aggregates of eosinY molecules. They lead to a kind of filter effect that lowers the photocurrent and efficiency. This effect has also been referred to as concentration quenching in some publications.[24,25] On the other hand, single eosinY molecules adsorbed on ZnO seem to have a high electron injection efficiency not only in the colloidal films, as seen in the results of the IMPS fits ($\Phi_{inj} = 1$), but also in the electrodeposited films. Current studies on the further development of electrodeposited ZnO/dye films are therefore focused on avoiding or removing dye aggregation in the film. First results show that the efficiency of the films can be enhanced significantly if the dye is removed from the ZnO by dilute KOH (aq) and readsorbing to the ZnO from ethanolic solution,[26] which strongly supports the conclusions of this study.

Conclusions

The comparison of electrochemically self-assembled and colloidal ZnO/eosinY films indicated that the electrodeposited films show faster electron transport and, in conjunction with their high dye concentration and low film thickness, a much more efficient electron collection. This is a very promising result of this study in view of an application of electrodeposited ZnO/dye hybrid films in dye-sensitized solar cells, especially flexible solar cells, where no high-temperature sintering can be applied. It also has been shown that the currently still low efficiency of cells based on these films is due to a low efficiency of electron injection from the dye into the ZnO. It is suggested that this low efficiency of electron injection is caused by the formation of dye aggregates in the film where a part of the dye molecules cannot inject electrons into ZnO. An improvement of the electron injection in the electrodeposited film can lead to significantly higher efficiencies than can be reached with colloidal ZnO films.

Acknowledgment. Financial support by the Industrial Technology Research Grant Program 2003 from NEDO (New Energy and Industrial Technology Development Organization of Japan, No. 01B64002C) and by a Grant-in-Aid for Scientific Research (A) from the Ministry of Education, Culture, Sports, Science and Technology of Japan (No. 15681005) is gratefully acknowledged. The stay of T.O. at Gifu University was made possible by a postdoctoral fellowship from JSPS (Japan Society for the Promotion of Science). We also thank Petra Cameron for assistance with the IMPS measurements.

References and Notes

(1) Yoshida, T.; Minoura, H. *Adv. Mater.* **2000**, *12*, 1219.

(2) Yoshida, T.; Tochimoto, M.; Schlettwein, D.; Wöhrle, D.; Sugiura, T.; Minoura, H. *Chem. Mater.* **1999**, *11*, 2657.

(3) Oekermann, T.; Yoshida, T.; Schlettwein, D.; Sugiura, T.; Minoura, H. *Phys. Chem. Chem. Phys.* **2001**, *3*, 3387.

(4) Yoshida, T.; Yoshimura, J.; Matsui, M.; Sugiura, T.; Minoura, H. *Trans. Mater. Res. Soc. Jpn.* **1999**, *24*, 497.

(5) Yoshida, T.; Terada, K.; Schlettwein, D.; Oekermann, T.; Sugiura, T.; Minoura, H. *Adv. Mater.* **2000**, *12*, 1214.

(6) Yoshida, T.; Oekermann, T.; Okabe, K.; Schlettwein, D.; Funabiki, K.; Minoura, H. *Electrochemistry* **2002**, *70*, 470.

(7) Yoshida, T.; Pauporté, T.; Lincot, D.; Oekermann, T.; Minoura, H. *J. Electrochem. Soc.* **2003**, *150*, C608.

(8) Peter, L. M.; Vanmaekelbergh, D. In *Advances in Electrochemical Science and Engineering*; Alkire, R. C., Kolb, D. M., Eds.; Wiley-VCH: Weinheim, 1999; Vol. 6.

(9) Södergren, S.; Hagfeldt, A.; Olsson, J.; Lindquist, S. E. *J. Phys. Chem.* **1994**, *95*, 5522.

(10) Vanmaekelbergh, D.; de Jongh, P. *J. Phys. Chem. B* **1999**, *103*, 747.

(11) Dloczik, L.; Ileperuma, O.; Lauermann, I.; Peter, L. M.; Ponomarev, E. A.; Redmond, G.; Shaw, N. J.; Uhlendorf, I. *J. Phys. Chem. B* **1997**, *101*, 10281.

(12) Schlichthörl, G.; Huang, S. Y.; Sprague, J.; Frank, A. J. *J. Phys. Chem. B* **1997**, *101*, 8141.

(13) Fisher, A. C.; Peter, L. M.; Ponomarev, E. A.; Walker, A. B.; Wijayantha, K. G. U. *J. Phys. Chem. B* **2000**, *104*, 949.

(14) Duffy, N. W.; Peter, L. M.; Rajapakse, R. M. G.; Wijayantha, K. G. U. *Electrochem. Commun*. **2000**, *2*, 658.

(15) Franco, G.; Peter, L. M.; Ponomarev, E. A. *Electrochem. Commun*. **1999**, *1*, 61.

(16) Vanmaekelbergh, D.; Iranzo Marin, F.; van de Lagemaat, J. *Ber. Bunsen-Ges. Phys. Chem.* **1996**, *100*, 616.

(17) Cao, F.; Oskam, G.; Meyer, G. J.; Searson, P. C. *J. Phys. Chem.* **1996**, *100*, 17021.

(18) Peter, L. M.; Wijayantha, K. G. U. *Electrochem. Commun.* **1999**, *1*, 576.

(19) Kronik, L.; Bachrach-Ashkenasy, N.; Leibovich, M.; Fefer, E.; Shapira, Y.; Gorer, S.; Hodes, G. *J. Electrochem. Soc.* **1998**, *145*, 1748.

(20) Nakade, S.; Kubo, W.; Saito, Y.; Kanzaki, T.; Kitamura, T.; Wada, Y.; Yanagida, S. J. *Phys. Chem. B* **2003**, *107*, 14244.

(21) Park, N. G.; Schlichthörl, G.; van de Lagemaat, J.; Cheong, H. M.; Mascarenhas, A.; Frank, A. J. *J. Phys. Chem. B* **1999**, *103*, 3308.

(22) Nakade, S.; Matsuda, M.; Kambe, S.; Saito, Y.; Kitamura, T.; Sakata, T.; Wada, Y.; Mori, H.; Yanagida, S. *J. Phys. Chem. B* **2002**, *106*, 10004.

(23) Vayssieres, L.; Hagfeldt, A.; Lindquist, S. E. *Pure Appl. Chem.* **2000**, *72*, 47.

(24) Tennakone, K.; Fernando, C. A. N.; Dewasurendra, M.; Kariapper, M. S.; Jayatissa, A. H. *J. Photochem.* **1987**, *37*, 257.

(25) Fernando, C. A. N. *Sol. Energy Mater. Sol. Cells* **1993**, *28*, 375.

(26) Yoshida, T.; Iwaya, M.; Ando, H.; Oekermann, T.; Nonomura, K.; Schlettwein, D.; Wöhrle, D.; Minoura, H. *Chem. Commun*. **2004**, 400.